ARTICLES

Craik–Criminale solutions and elliptic instability in nonlinear-reactive closure models for turbulence

Bruce R. Fabijonas[a)]
Department of Mathematics, Southern Methodist University, Dallas, Texas 75275-0156

Darryl D. Holm[b)]
Theoretical Division and Center for Nonlinear Studies, Los Alamos National Laboratory, Los Alamos, New Mexico 87545
and Mathematics Department, Imperial College of Science, Technology and Medicine, London SW7 2AZ, United Kingdom

(Received 20 March 2003; accepted 13 November 2003; published online 6 February 2004)

The Craik–Criminale class of exact solutions is examined for a nonlinear-reactive fluids theory that includes a family of turbulence closure models. These may be formally regarded as either large eddy simulation or Reynolds-averaged Navier–Stokes models of turbulence. All of the turbulence closure models in the class under investigation preserve the existence of elliptic instability, although they shift its angle of critical stability as a function of the rotation rate Ω of the coordinate system, the wave number β of the Kelvin wave, and the model parameter α, the turbulence correlation length. Elliptic instability allows a comparison among the properties of these models. It is emphasized that the physical mechanism for this instability is not wave–wave interaction, but rather wave, mean-flow interaction as governed by the choice of a model's nonlinearity. © *2004 American Institute of Physics.* [DOI: 10.1063/1.1638750]

I. INTRODUCTION

The fully nonlinear ''elliptic instability'' rapidly generates three-dimensional flows in regions of two-dimensional, elliptical flowlines, e.g., in an elliptical vortex column, or vortex tube. This instability is triggered when it becomes possible for a wave packet propagating in three dimensions to draw energy from an elliptical column of mean vorticity. The mechanism for elliptic instability is a parametric resonance in the wave, mean-flow interactions. The instability is fundamentally three-dimensional, and its average maximum growth rate is proportional to the mean strain rate, or equivalently, the eccentricity of the elliptical flowlines. The mechanism for elliptic instability is the same as that for critical layer absorption.[1] Laboratory experiments and numerical modeling show that elliptic instability quickly breaks down the elliptical vortex columns by producing complicated flows, which themselves break down into small-scale disorder. As a result, elliptic instability is a natural candidate for studying mechanisms involved in the onset and dynamics of turbulence, in which the intermittent stretching of vortex filaments by rapid three-dimensional fluctuations is a fundamental process.

Thus, elliptic instability is the nonlinear mechanism by which vorticity creates three-dimensional instabilities in swirling two-dimensional flows. In the classic paradigm, energy in an elliptic columnar vortex is transferred to a traveling Kelvin wave whose wave vector is fully three-dimensional. A detailed review of elliptic instability can be found in Ref. 2. The topic was first investigated by Lord Kelvin[3] in 1887 for a circular vortex column and then was generalized to elliptical vortex columns almost a century later by Bayly.[4] Both investigations considered the stability of a traveling wave for the equations of motion *linearized* about the rotating column of fluid. The groundbreaking work of Craik and Criminale[5] showed that the sum of a rotating column of fluid and a traveling Kelvin wave together with any number of its harmonics is an *exact solution* to the nonlinear Navier–Stokes (NS) equations. These exact nonlinear solutions are called Craik–Criminale (CC) solutions.

The CC class of exact NS solutions provides a means of analyzing the three-dimensional nonlinear dynamics of elliptic instability. These exact solutions show that elliptic instability is generated by wave, mean-flow interaction via the nonlinear term in the NS equations. Thus, elliptic instability is a fundamental nonlinear mechanism in the dynamics of turbulence. It seems reasonable to compare computational models of turbulence in the light of whether they realistically incorporate the effects of elliptic instability. In this paper, we extend the literature of the CC flows by considering the elliptic instabilities allowed by a nonlinear-reactive (as opposed to nonlinear-dissipative) fluid theory that includes a new class of one-point turbulence closure models whose derivation by Lagrangian averaging alters the nonlinearity of

a)Electronic mail: bfabi@mail.smu.edu
b)Electronic mail: dholm@lanl.gov

the NS equations. This class of models was identified earlier and studied analytically and numerically in a series of papers; see Refs. 6 and 7 and references therein. The question that we shall investigate here is, "How do these nonlinear-reactive turbulence closure models deal with elliptic instability?" The answer to this question for each turbulence model in this class allows us to compare the models according to how their exact nonlinear solutions describe, or alter, the fundamental NS elliptic instability. Formally, the mathematical analysis we present applies equally well to turbulence closure models derived by either the RANS (Reynolds-averaged Navier–Stokes) approach or LES (large eddy simulations).

The CC class of solutions have recently been revisited by the present authors.[8] It was shown that the CC class of exact solutions persists for the Lagrangian-averaged Navier–Stokes-alpha (LANS-α) model, a new closure model for incompressible turbulence that was introduced in Refs. 9 and 10. This paper investigates the CC solutions of the LANS-α model in detail together with the effects of rotation and extends the CC analysis for several other constitutive models for turbulence closure in a class of nonlinear-reactive fluids.

Nonlinear exact CC solutions of the NS equations: The CC class of nonlinear exact solutions decomposes both fluid velocity and pressure into the sum of two terms, as $\mathbf{u}=\mathbf{u}_0+\mathbf{u}_1$ and $p=p_0+p_1$. Here the base flow $\{\mathbf{u}_0,p_0\}$ is an *exact* solution to the equations of motion in an unbounded physical domain linear in the spatial coordinate. Consequently, in the CC solutions, both of the pairs $\{\mathbf{u}_0,p_0\}$ and $\{\mathbf{u},p\}$ are exact solutions to the nonlinear equations. While the base flow in the CC decomposition is an exact solution, the disturbance $\{\mathbf{u}_1,p_1\}$ by itself is, in general, only a solution of the equations linearized about the base flow $\{\mathbf{u}_0,p_0\}$.

The CC solutions consider the disturbance $\{\mathbf{u}_1,p_1\}$ in the form of a traveling wave,

$$\begin{aligned}\mathbf{u}_1&=\Re\{\mu\mathbf{a}(t)e^{i\psi}\},\\ p_1&=\Re\{i\mu p_{11}(t)e^{i\psi}+\mu^2 p_{12}(t)e^{2i\psi}\},\end{aligned}\tag{1}$$

where the amplitude $\mathbf{a}(t)$ depends only on time and the phase $\psi(\mathbf{x},t)=\beta\mathbf{k}(t)\cdot\mathbf{x}+\delta(t)$ is linear in the spatial coordinate. The phase shift $\delta(t)$ may also be regarded as arising from a time-dependent shift of the origin of coordinates. The scaling parameters μ and β are chosen so the initial conditions may be normalized as $|\mathbf{k}(0)|=1$ and $|\mathbf{a}(0)|=1$. The parameter β can be viewed as the product of the wave number and the relative scale of lengths between the base flow and the Kelvin wave. The base flow is linear in the spatial coordinates, $\mathbf{u}_0=\mathcal{S}(t)\cdot\mathbf{x}+\mathbf{U}(t)$, where $\mathcal{S}\cdot\mathbf{x}=S_{ij}x_j$ is the action of the matrix $\mathcal{S}(t)$ on the vector $\mathbf{x}=[x_1,x_2,x_3]^T$ from the left and $\mathbf{U}(t)$ is the instantaneous velocity at the origin. The construction method is one in which the Kelvin wave does not alter the evolution of the base flow. The classic problem of elliptic instability is found in this class of solutions,

$$\mathcal{S}=\begin{pmatrix}0 & -1+\gamma & 0\\ 1+\gamma & 0 & 0\\ 0 & 0 & 0\end{pmatrix},\quad \mathbf{U}=\mathbf{0}.\tag{2}$$

Here, the base flow in this case is a rigidly rotating column of fluid whose flowlines are ellipses with eccentricity γ. The extreme values are circles ($\gamma=0$) and simple shear flows ($\gamma\to1^-$).

Outline: We begin by reviewing the classic CC solutions for the NS equations in Sec. II. In particular, we shall review the case of elliptic instability. Section III examines this class of solutions and elliptic instability for certain turbulence closure models, regarded as "constitutive laws" for nonlinear-reactive fluids that include the LANS-α model. In Sec. IV, we perform a detailed examination of the CC class of exact solutions and elliptic instability in the LANS-α model. We then examine the class of CC solutions in full generality for each of the other turbulence closure models in Sec. V. We summarize our results in Sec. VI. Overall, we conclude that the study of exact nonlinear CC solutions for these models defines sharp distinctions among them. For example, the CC solutions for these models provide detailed comparisons of their principal critical angles of instability and maximum growth rates, as functions of their parameters. The CC solutions for these models also determine to what extent each model preserves the fundamental attributes of the elliptic instability for NS. Thus, elliptic instability analysis allows a fully nonlinear comparison of turbulence closure models on the basis of the specific and fundamental physical mechanism of their wave, mean-flow interaction, rather than on the basis of tensor transformation properties, or other generalities.

II. REVIEW OF CC SOLUTIONS OF THE NAVIER–STOKES EQUATIONS

We begin with a review of the classic CC results for the NS equations

$$\partial_t\mathbf{u}+\mathbf{u}\cdot\nabla\mathbf{u}+\nabla p+2\boldsymbol{\Omega}\times\mathbf{u}-\nu\Delta\mathbf{u}=\mathbb{F},\tag{3}$$

in which preservation of incompressibility, $\operatorname{div}\mathbf{u}=0$, determines the pressure, p. Here, $\mathbb{F}$ represents the sum of all external body forces. Clearly, $\mathbf{u}_0=\mathcal{S}(t)\cdot\mathbf{x}+\mathbf{U}(t)$, together with the pressure $p_0(\mathbf{x},t)=\mathbf{x}\cdot\mathcal{Q}(t)\cdot\mathbf{x}+\pi(t)\mathbf{x}$ is a solution in an unbounded domain. The matrix $\mathcal{S}(t)$ is a time dependent matrix with zero trace such that

$$d_tS_{ij}+S_{im}S_{mj}+2\epsilon_{imk}\Omega_mS_{kj}=M_{ij}.\tag{4}$$

Here, d_t denotes full time derivative, and $M(t)$ is a symmetric matrix defined as $M_{ij}=-\partial_i\partial_j\mathbb{P}$, where

$$\mathbb{P}=-\int^{\mathbf{x}}\mathbb{F}\cdot d\mathbf{x}+p_0(\mathbf{x},t)+(d_t\mathbf{U}+\mathcal{S}\cdot\mathbf{U}+2\boldsymbol{\Omega}\times\mathbf{U})\cdot\mathbf{x}.\tag{5}$$

A typical solution approach is to choose a matrix $\mathcal{S}(t)$ for which the left-hand side of Eq. (4) is symmetric. Then, the corresponding pressure $p_0(\mathbf{x},t)$ is determined *a posteriori* by Eq. (5). We may nondimensionalize the NS equations by using the variables $\mathbf{x}'=\mathbf{x}/l$, $t'=|\omega|t$, $\mathbf{u}=\mathbf{u}/|\omega|l$, $\boldsymbol{\Omega}'=\boldsymbol{\Omega}/|\omega|$, where l is a typical length scale and $\boldsymbol{\omega}=\operatorname{curl}\mathbf{u}_0$ is the vorticity of the flow $\mathbf{u}_0$. After dropping primes from the notation, Eq. (3) reappears in nondimensional form with ν replaced by $\nu/|\omega|$. Furthermore, in nondimensional form, Ω is now interpreted as a signed inverse Rossby number. The

equations for the amplitude $\mathbf{a}$ and the phase ψ are obtained upon making the CC substitution $\mathbf{u}=\mathbf{u}_0+\mathbf{u}_1$ and $p=p_0+p_1$ into Eq. (3), where $\mathbf{u}_1$ and p_1 are given in Eq. (1) and by collecting on terms linear and constant in $\mathbf{x}$, respectively,

$$\partial_t(\mathbf{k}\cdot\mathbf{x})+\mathbf{k}\cdot\mathcal{S}\cdot\mathbf{x}=0, \tag{6}$$

$$\frac{\mathrm{d}\mathbf{a}}{\mathrm{d}t}+i(d_t\delta+\beta\mathbf{k}\cdot\mathbf{U})\mathbf{a}+\mathcal{S}^T\cdot\mathbf{a}+\mathbf{\Pi}\times\mathbf{a}+E_\omega|\mathbf{k}|^2\mathbf{a}-\beta p_{11}\mathbf{k}=\mathbf{0}, \tag{7}$$

$$p_{12}=0, \tag{8}$$

$$\mathbf{a}\cdot\mathbf{k}=0. \tag{9}$$

Here, $\mathbf{\Pi}=\mathrm{curl}\,\mathbf{u}_0+2\mathbf{\Omega}$ is the total vorticity of the system, that is, the vorticity of the base flow, plus that of the rotating coordinate system, and $E_\omega=\nu\beta^2/|\omega|$ is the vorticity-based Ekman number. Note that we have used the identity $\mathrm{curl}\,\mathbf{u}_0\times\mathbf{a}=(\mathcal{S}-\mathcal{S}^T)\cdot\mathbf{a}$ for reasons we explain below. The transversality condition in Eq. (9) arises from the incompressibility condition. This transversality is why the term $\mathbf{u}_1\cdot\nabla\mathbf{u}_1$ quadratic in the disturbance velocity vanishes. We emphasize that CC solutions are exact, nonlinear solutions of the NS equations because the nonlinear wave–wave interaction vanishes exactly. This transversality condition fails when one tries to add two Kelvin waves where the phases are not rationally related. Without loss of generality, we may choose the kinematic phase relation, $d_t\delta+\beta\mathbf{k}\cdot\mathbf{U}=0$, where $\mathbf{U}(t)$ denotes the coordinate-independent contribution of $\mathbf{u}_0$. By doing this, the term $\delta(t)$ exactly balances the instantaneous velocity of the base flow at the origin, $\mathbf{U}(t)$. Then, we see from Eq. (7) that we can assume that $\mathbf{a}(t)$ is a real-valued function. The equation for the wave vector $\mathbf{k}(t)$ obtained from the phase equation (6) is the transport equation,

$$\frac{\mathrm{d}\mathbf{k}}{\mathrm{d}t}+\mathcal{S}^T\cdot\mathbf{k}=\mathbf{0}. \tag{10}$$

Since $\mathrm{d}\mathbf{k}/\mathrm{d}t+\mathcal{S}^T\cdot\mathbf{k}$ is the total time derivative of $\mathbf{k}$ in a Galilean frame moving with the base flow $\mathbf{u}_0$, we see that the wave vector $\mathbf{k}$ is frozen into the base flow. Equation (7) states that the evolution of the real amplitude $\mathbf{a}$ in this frame undergoes rotation by the total vorticity of the base flow, as it decays exponentially with viscosity. In fact, the change of variables

$$\mathbf{a}=\tilde{\mathbf{a}}\exp\left(-E_\omega\int_0^t|\mathbf{k}(\hat{t})|^2\,d\hat{t}\right) \tag{11}$$

will transform away viscosity from the problem. The pressure term p_{11} can be expressed in terms of $\mathbf{a}$ and $\mathbf{k}$ by taking the dot product of Eq. (7) with $\mathbf{k}$ and recalling that $\mathbf{a}\cdot\mathbf{k}$ is an integral of motion. Consequently, one finds the pressure relation,

$$\beta p_{11}=\frac{\mathbf{a}\cdot(\mathcal{S}+\mathcal{S}^T)\cdot\mathbf{k}+\mathbf{\Pi}\times\mathbf{a}\cdot\mathbf{k}}{|\mathbf{k}|^2}. \tag{12}$$

Thus, Eq. (7) can be expressed as

$$\frac{\mathrm{d}\mathbf{a}}{\mathrm{d}t}=\mathcal{N}(t)\cdot\mathbf{a}, \tag{13}$$

where $\mathcal{N}$ is a 3×3 matrix which may have some parametric dependence, as well. Earlier, we noted that both $\mathbf{u}_0$ and the sum $\mathbf{u}_0+\mathbf{u}_1$ are exact solutions to the nonlinear equations. However, the disturbance velocity $\mathbf{u}_1$ by itself is, in general, only a solution to Eq. (3) linearized about $\mathbf{u}_0$. As an important exception, in a rotating coordinate system ($\mathbf{\Omega}\neq\mathbf{0}$), the velocity $\mathbf{u}_1$ by itself is also an exact solution, since this scenario corresponds to $\mathbf{u}_0=\mathcal{R}\cdot\mathbf{x}$ in a nonrotating frame, where $\mathcal{R}$ is rigid body rotation about the z axis; cf. Ref. 12. The specific problem of elliptic instability in the NS equations using the base flow $\mathbf{u}_0=\mathcal{S}\cdot\mathbf{x}$ as in Eq. (2) was first investigated by Bayly[4] for $\Omega=0$, by Craik[11] for $\Omega\neq0$, and later by others.[12–17] Equation (10) for the wave vector $\mathbf{k}(t)$ has an analytical solution for all elliptical eccentricities γ, namely

$$\mathbf{k}=[\sin\theta\cos(\chi(t)),\kappa\sin\theta\sin(\chi(t)),\cos\theta]^T, \tag{14}$$

where $\kappa^2=(1-\gamma)/(1+\gamma)$, $\chi(t)=t\sqrt{1-\gamma^2}$, and θ is the polar angle $\mathbf{k}$ makes with the axis of rotation. For circular flowlines, $\gamma=0$, Eq. (7) for the wave amplitude $\mathbf{a}$ also has an analytical solution: $\mathbf{a}=c_1\mathbf{a}_1(t)+c_2\mathbf{a}_2(t)+c_3\mathbf{a}_3(t)$, where c_1,c_2,c_3, are constants and

$$\mathbf{a}_1(t)=\cos(\xi(t)+\phi)\mathbf{k}_{\perp1}+\sin(\xi(t)+\phi)\mathbf{k}_{\perp2}, \tag{15}$$

$$\mathbf{a}_2(t)=\sin(\xi(t)+\phi)\mathbf{k}_{\perp1}-\cos(\xi(t)+\phi)\mathbf{k}_{\perp2}, \tag{16}$$

$$\mathbf{a}_3(t)=\mathbf{e}_z. \tag{17}$$

Also, $\mathbf{k}_{\perp1}=[\cos\theta\cos(\chi(t)),\cos\theta\sin(\chi(t)),-\sin\theta]^T$, $\mathbf{k}_{\perp2}=[\sin(\chi(t)),-\cos(\chi(t)),0]^T$, $\xi(t)=2t(1+\Omega)\cos\theta$, and ϕ is an arbitrary phase. For elliptical flowlines with eccentricity γ, the solution to Eq. (7) for the CC wave amplitude $\mathbf{a}$ must be determined numerically. Because the wave vector $\mathbf{k}$ is periodic, Eq. (13) for the amplitude $\mathbf{a}$ satisfies a Floquet problem.[18] Thus, integration of Eq. (13) over one period of $\mathbf{k}$ will determine the Lyapunov growth rate of $\mathbf{a}$, if any such growth occurs. These growth rates are determined by computing the eigenvalues ρ_i of the monodromy matrix $\mathcal{P}(\tau_p)$, where $\mathcal{P}(0)=\mathrm{diag}\{1,1,1\}$,

$$\frac{\mathrm{d}\mathcal{P}}{\mathrm{d}t}=\mathcal{N}\cdot P, \tag{18}$$

and τ_p is the period of $\mathcal{N}$; in this case, $\tau_p=2\pi/\sqrt{1-\gamma^2}$, the period of $\mathbf{k}$. Once computed, the Lyapunov growth rates are given by $\sigma_g=\max_i[\ln(\Re\{\rho_i\})]/\tau_p$. The growth rates for the Euler equations are shown in Fig. 1 for $\Omega=0$. We see from this figure that the amplitude $\mathbf{a}$ has an exponential growth rate for certain orientations of the wave vector and for all nonzero eccentricities. We emphasize that the CC solution is an exact solution to the nonlinear NS equations for all parameter values. A CC solution is said to be unstable, if the magnitude of its amplitude $\mathbf{a}$ is unbounded as $t\to\infty$.

CC solutions of NS for circular flowlines: The circular case $\gamma=0$ can be treated analytically. One may construct the monodromy matrix explicitly from the solutions in Eqs. (15)–(17). For the initial condition $\mathcal{P}(0)=\mathrm{diag}\{1,1,1\}$, we find the monodromy matrix,

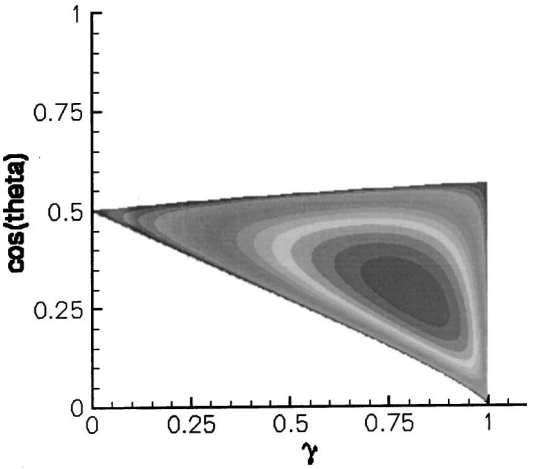

FIG. 1. Parameter plane for elliptic instability in NS equations for $\Omega=0$. For $\gamma=0$, the Kelvin wave is periodic in time with period $\pi/\cos\theta$; for values of γ, $\cos\theta$ which fall into the white region for $\gamma>0$, the Kelvin wave is quasiperiodic, that is, the periods of **a** and **k** are incommensurate; for the remaining region, the Kelvin wave has an exponentially growing amplitude. The maximum growth rate is 0.36 at $\cos\theta=0.29$ and $\gamma=0.81$.

$$\mathcal{P}(\tau_p) = \begin{pmatrix} \cos(\xi(2\pi)) & \cos\theta\sin(\xi(2\pi)) & 0 \\ -\sin(\xi(2\pi))/\cos\theta & \cos(\xi(2\pi)) & 0 \\ \tan\theta(1-\cos(\xi(2\pi))) & -\sin\theta\sin(\xi(2\pi)) & 1 \end{pmatrix}. \tag{19}$$

The eigenvalues are $\rho_{1,2}=\exp(\pm i\xi(2\pi))$, $\rho_3=1$, and we conclude that traveling waves in circular NS flows are stable. The parameter values for critical stability, that is, the parameter values at which exponentially growing amplitudes will appear for nonzero values of γ, occur when $|\rho_i|=1$, $i=1,2,3$, or equivalently, $\xi(2\pi)=m\pi$, where m is any integer. As argued by Bayly,[4] the evenness of $\beta p_{11}\mathbf{k}$ as a function of **k** in Eq. (7) implies that the eigenvalues of the monodromy matrix, if real and unequal, must be positive. This eliminates the odd choices of m. The case $m=0$ cannot be analyzed using Floquet theory since the equations are no longer periodic. Therefore, the critical stability points are determined by $\xi(2\pi)=2n\pi$, or equivalently,

$$\cos\theta=\pm\frac{n}{2(\Omega+1)}, \quad n=1,2,3,\ldots. \tag{20}$$

The critical angle of $\cos\theta=1/2$ for $\Omega=0$ is seen in Fig. 1. Since $|\cos\theta|\leqslant 1$, it follows from Eq. (20) that no critical stability points exist for $-\frac{1}{2}<\Omega+1<\frac{1}{2}$. Computation of the unstable region on an extremely fine grid yields fingers for $\Omega>0$ and $\Omega<-2$. These fingers have growth rates about five or six orders of magnitude smaller than in the principal region. Figure 2 shows one such simulation for the Euler equations. The fingers were first discussed by Miyazaki.[19] We are certain that the fingers are not numerical artifacts, since they are not randomly distributed in the parameter plane. Rather, they follow specific paths. We claim that these fingers correspond to solutions of Eq. (20) for $n>1$. The fingers are numerically resolvable for $\Omega>0$ and $\Omega<-2$.

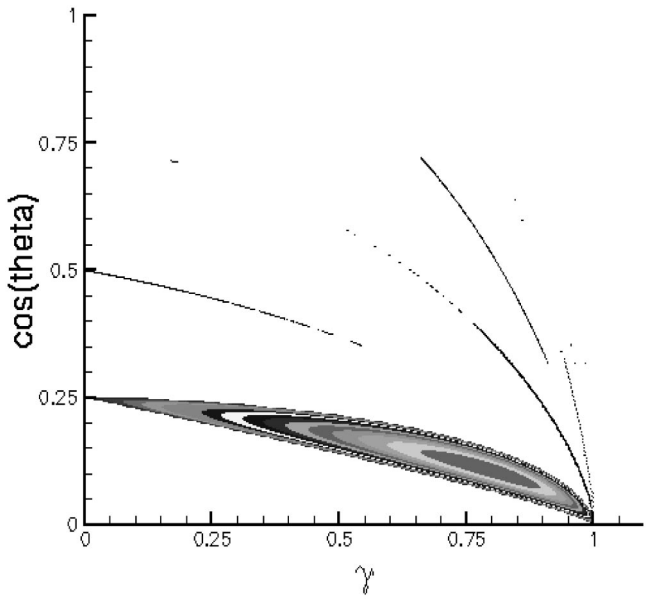

FIG. 2. Instability domain for $E_\omega=0$, $\Omega=1.0$ computed on an extremely fine grid aimed at capturing the predicted fingers. The white background represents regions for which $\sigma_g<10^{-10}$. The principal finger emanates from $\cos\theta=1/[2(1+\Omega)]$, the second finger clearly emanates from $\cos\theta=2/[2(1+\Omega)]$, and the third finger appears to emanate from $\cos\theta=3/[2(1+\Omega)]$. The remaining few points seen correspond to the fourth and fifth fingers.

This claim is contrary to previous thought.[2,4,8,15] We emphasize that these fingers are physically insignificant in the NS equations. However, they will be of importance in the LANS-α model discussed in the next section. Finally, one can determine the average value of the growth rate, to leading order in $\gamma\ll 1$, as in Ref. 15 by computing

$$\overline{\sigma_g}\equiv\frac{1}{\xi(2\pi)}\int_0^{\xi(2\pi)}\frac{1}{|\mathbf{a}|^2}\frac{d}{dt}\left(\frac{1}{2}|\mathbf{a}|^2\right)dt = \frac{9}{16}\gamma\times\frac{(3+2\Omega)^2}{9(1+\Omega)^2}+O(\gamma^2). \tag{21}$$

III. CC SOLUTIONS FOR ROTATING NONLINEAR-REACTIVE FLUIDS

A. Navier–Stokes nonlinear-reactive models

The turbulence closure models may be expressed as a set of partial differential equations for the divergenceless velocity of the fluid, $\mathbf{u}(\mathbf{x},t)$,

$$\frac{d\mathbf{u}}{dt}-\nu_T\Delta\mathbf{u}+\nabla p+2\boldsymbol{\Omega}\times\mathbf{u}+\operatorname{div}\sigma=0 \tag{22}$$

with $\nabla\cdot\mathbf{u}=0$. Here $d/dt=\partial_t+\mathbf{u}\cdot\nabla$ is the material time derivative following the resolved flow velocity, or mean velocity, **u**, and ν_T is the eddy viscosity. The nonlinear stress tensor σ we shall consider is a recent extension of the subgrid-stress tensor for turbulence that was introduced by Speziale[20] to account for Reynolds-stress relaxation effects and the response to rotational strain rates in turbulence. In the following reactive closure model for the Reynolds stress, we introduce a parameter α which will later be defined as a

turbulence correlation length. One obtains the model introduced by Speziale[20] for Reynolds-averaged Navier–Stokes (RANS) modeling of turbulence based on nonlinear constitutive relations, by setting the parameter $\alpha^2 \to 0$,

$$\frac{1}{C_0 \ell^2}\sigma_{ij} = \frac{-1}{\theta_0}(1-\alpha^2\Delta)e_{ij} + C_1 e_{ik}e_{kj} + C_2(e_{ik}\omega_{kj} - \omega_{ik}e_{kj}) + C_3\omega_{ik}\omega_{kj} + C_4(\partial_t e_{ij} + u^k \partial_k e_{ij}). \tag{23}$$

As usual, one sums over repeated indices. The tensors e_{ij} and ω_{ij} with $i,j = 1,2,3$ are, respectively, the mean strain rate and mean vorticity,

$$e_{ij} = \tfrac{1}{2}(u_{j,i} + u_{i,j}) = \tfrac{1}{2}(\nabla \mathbf{u}^T + \nabla \mathbf{u})_{ij}, \quad \omega_{ij} = \tfrac{1}{2}(u_{j,i} - u_{i,j}) = \tfrac{1}{2}(\nabla \mathbf{u}^T - \nabla \mathbf{u})_{ij}. \tag{24}$$

Suppressing indices, we may rewrite the symmetric Reynolds-stress tensor (23) as

$$\frac{\sigma}{C_0 \ell^2} = -(1-\alpha^2\Delta)\frac{e}{\theta_0} + C_1 e^2 + C_2(e\cdot\omega - \omega\cdot e) + C_3\omega^2 + C_4\frac{de}{dt}. \tag{25}$$

The parameters C_m, $m = 1,\ldots,4$, in Eq. (25) are four dimensionless constants that model nonlinear (C_1, C_3, C_3) and reactive (C_4) effects in turbulence, θ_0 is a dissipation time scale, and $C_0\ell^2$ and α^2 are squares of length scales. In the linear, nonreactive limit, $C_m \to 0$, $m = 1,\ldots,4$, one recovers the hyperviscosity model of turbulence for $\alpha^2 \neq 0$. This, in turn, becomes the usual eddy viscosity model by also setting $\alpha^2 \to 0$. When both $C_4 = 0$ and $\alpha^2 = 0$, the stress tensor in Eq. (25) takes the form $\sigma_{ij} = A_{ijkl}u_{k,l}$ of an ''anisotropic eddy-viscosity model'' (where A_{ijkl} depends algebraically on the mean-velocity gradients). When $C_4 \neq 0$ and $\alpha^2 = 0$, Eq. (25) reduces to the Speziale model, which represents a class of nonlinear-reactive models, which have wave-number-independent damping instead of ordinary Navier–Stokes viscosity. For example, setting $(C_1, C_2, C_3) = (C_4/2)(0,1,0)$ with $\alpha^2 = 0$ in Eq. (25) yields the stress tensor for second-grade fluids.[21] Thus, both the nonlinear-reactive constitutive models of Rivlin–Erickson,[22] Noll–Truesdell[23] and the RANS turbulence closure models of Speziale[20] may be recovered by setting $\alpha^2 = 0$ in Eq. (25). The analogies between the mean turbulent flow of a Newtonian fluid and the laminar flow of a non-Newtonian fluid have been a perennial subject of discussion at least since Rivlin.[24] One recurring topic in this discussion has been the question of material frame indifference (MFI), defined as form invariance of the Reynolds-stress divergence under arbitrary time-dependent rotations and translations of the reference frame. In turbulence, MFI is applied modulo the Coriolis force, so that rotation enters solely through the total mean vorticity tensor, $\overline{W}_{ij} = \omega_{ij} + 2\epsilon_{ijk}\Omega^k$. The application of MFI restricts the allowable form of the Reynolds-stress tensors for RANS turbulence models in Eq. (25) by requiring $C_2 = C_4/2$ and $C_3 = 0$. The remaining parameter C_1 is left unrestricted by MFI, because the strain-rate tensor e is invariant under the MFI transformations. In the present work, we shall consider both $C_4 \neq 0$ and $\alpha^2 \neq 0$ in the reactive stress tensor (25). In this case, we emphasize that the parameter $\alpha^2 \neq 0$ corresponds to ordinary eddy viscosity, not hyperviscosity. Later, we shall obtain a simplification by relating $C_4 \neq 0$ and $\alpha^2 \neq 0$ as $\alpha^2 = C_0\ell^2 C_4/2$. It is immaterial for the motion equation (22) whether one uses the symmetric stress tensor, σ, or its deviatoric (*traceless*) component, $\sigma - \frac{1}{3}\mathrm{Id}\,\mathrm{tr}(\sigma)$, since the difference merely adjusts the pressure, p, which is determined by preservation of the divergence-free condition, $\mathrm{div}\,\mathbf{u} = 0$. The mass density has been set equal to unity.

We may summarize this discussion of the nonlinear, reactive and dissipative RANS turbulence closure models represented by Eq. (22) with Reynolds-stress tensor (25), by distinguishing the following subcases.

(1) Navier–Stokes: $C_0 = 0$.
(2) Isotropic eddy viscosity: $C_m = 0$ and $\alpha^2 = 0$.
(3) Anisotropic eddy viscosity: $C_1, C_2, C_3 \neq 0$, $C_4 = 0$ and $\alpha^2 = 0$.
(4) Isotropic eddy hyperviscosity: $C_m = 0$ and $\alpha^2 \neq 0$.
(5) Anisotropic eddy viscosity, isotropic hyperviscosity: $C_1, C_2, C_3 \neq 0$, $C_4 = 0$ and $\alpha^2 \neq 0$.
(6) Speziale:[20] $C_m \neq 0$ and $\alpha^2 = 0$ (reactive and damped, not actually viscous).
(7) Present work: $C_m \neq 0$ and $\alpha^2 \neq 0$ (reactive, damped and viscous, *not* hyperviscous).

As we have discussed, MFI of the Reynolds-stress tensor (25) would require certain restrictions among the parameters C_m. However, to make the analysis that follows of the Craik–Criminale solutions of Eq. (22) as broad as possible, we shall leave the parameters C_m free and unrestricted.

B. Recasting the Navier–Stokes nonlinear-reactive models

To facilitate the Craik–Criminale analysis in the next section, we shall recast the stress tensor in Eq. (25) in terms of the mean velocity gradient. We begin by rewriting Eq. (25) equivalently as

$$\begin{aligned}\frac{\sigma}{C_0\ell^2} + (1-\alpha^2\Delta)\frac{e}{\theta_0} - C_4\frac{de}{dt} &= C_1 e^2 + C_2(e\cdot\omega - \omega\cdot e) + C_3\omega^2 \\ &= \left(\frac{C_1}{4} + \frac{C_3}{4}\right)\nabla\mathbf{u}^T\cdot\nabla\mathbf{u}^T + \left(\frac{C_1}{4} + \frac{C_2}{2} - \frac{C_3}{4}\right)\nabla\mathbf{u}\cdot\nabla\mathbf{u}^T \\ &\quad + \left(\frac{C_1}{4} + \frac{C_3}{4}\right)\nabla\mathbf{u}\cdot\nabla\mathbf{u} + \left(\frac{C_1}{4} - \frac{C_2}{2} - \frac{C_3}{4}\right)\nabla\mathbf{u}^T\cdot\nabla\mathbf{u}.\end{aligned} \tag{26}$$

Computing divergences and using $\mathrm{div}\,\mathbf{u} = 0$ yields the following three useful identities:

$$\mathrm{div}\,2e = \Delta\mathbf{u}, \quad \mathrm{div}(\nabla\mathbf{u}^T\cdot\nabla\mathbf{u}^T) = \nabla\tfrac{1}{2}\mathrm{tr}(\nabla\mathbf{u}\cdot\nabla\mathbf{u}), \tag{27}$$

and

$$\operatorname{div} 2\frac{de}{dt} = -\Delta\frac{d\mathbf{u}}{dt} + \operatorname{div}\left(\nabla\mathbf{u}\cdot\nabla\mathbf{u} + \frac{1}{2}\nabla\mathbf{u}\cdot\nabla\mathbf{u}^T - \frac{1}{2}\nabla\mathbf{u}^T\cdot\nabla\mathbf{u}\right). \tag{28}$$

Hence, the divergence $\operatorname{div}(\nabla\mathbf{u}^T\cdot\nabla\mathbf{u}^T)$ may be absorbed into the pressure gradient. The other divergence terms arising from $\operatorname{div}\sigma$ are not gradients, and they may be rearranged into an *equivalent* version of the motion equation (22) for nonlinear-reactive fluids in a rotating frame as

$$\left(1 - C_0\ell^2\frac{C_4}{2}\Delta\right)\frac{d\mathbf{u}}{dt} = \left(\nu_T + \frac{C_0\ell^2}{2\theta_0}(1-\alpha^2\Delta)\right)\Delta\mathbf{u} - \nabla p - 2\boldsymbol{\Omega}\times\mathbf{u} - C_0\ell^2\operatorname{div}\tau, \tag{29}$$

with $\operatorname{div}\mathbf{u} = 0$ and stress divergence,

$$\operatorname{div}\tau = \operatorname{div}(b_1\nabla\mathbf{u}\cdot\nabla\mathbf{u} + b_2\nabla\mathbf{u}\cdot\nabla\mathbf{u}^T + b_3\nabla\mathbf{u}^T\cdot\nabla\mathbf{u}). \tag{30}$$

In components, this stress divergence relation is expressed as

$$(\operatorname{div}\tau)_i = \partial_j\tau_{ij} = \partial_j(b_1u_{i,k}u_{k,j} + b_2u_{i,k}u_{j,k} + b_3u_{k,i}u_{k,j}). \tag{31}$$

After absorbing $\operatorname{div}(\nabla\mathbf{u}^T\cdot\nabla\mathbf{u}^T)$ into the pressure gradient, the resulting stress tensor τ is no longer symmetric. However, one fewer constant is needed in specifying this version of the nonlinear-reactive fluid model. The relations between constants b_n, $n=1,2,3$, in Eq. (30) and C_m, $m=1,2,3,4$, in Eq. (23) are given by

$$b_1 = \frac{C_1}{4} + \frac{C_3}{4} + \frac{C_4}{2}, \quad C_1 = 2b_1 + b_2 + b_3 - C_4,$$

$$b_2 = \frac{C_1}{4} + \frac{C_2}{2} - \frac{C_3}{4} + \frac{C_4}{4}, \quad C_2 = b_2 - b_3 - \frac{1}{2}C_4,$$

$$b_3 = \frac{C_1}{4} - \frac{C_2}{2} - \frac{C_3}{4} - \frac{C_4}{4}, \quad C_3 = 2b_1 - b_2 - b_3 - C_4. \tag{32}$$

C. Outlook: CC solutions for nonlinear-reactive fluid motion

In what follows, we shall analyze exact nonlinear CC solutions of Eq. (29) for incompressible nonlinear-reactive fluid motion with stress tensor in Eq. (30). For this, we shall choose three special cases of the coefficients C_m, $m=1,\ldots,4$, in stress tensor (25), or equivalently, the coefficients b_i, $i=1,2,3$, in stress tensor (30), subject to the relation

$$\alpha^2 = C_0\ell^2C_4/2, \tag{33}$$

which unifies the Helmholtz operations in Eq. (29). These three choices are, as follows, all with $\nabla\cdot\mathbf{u}=0$ and definition $\mathbf{v}\equiv(1-\alpha^2\Delta)\mathbf{u}$.

(1) LANS-α model: $(C_1,C_2,C_3) = (C_4/2)\,(0,1,0)$ and $(b_1,b_2,b_3) = (C_4/2)\,(1,1,-1)$ expressed as

$$\frac{\partial\mathbf{v}}{\partial t} + (\mathbf{u}\cdot\nabla)\mathbf{v} + (\nabla\mathbf{u})^T\cdot\mathbf{v} + 2\boldsymbol{\Omega}\times\mathbf{u} + \nabla\left(p - \frac{1}{2}|\mathbf{u}|^2 - \frac{1}{2}\alpha^2|\nabla\mathbf{u}|^2\right) = \nu\Delta\mathbf{v}. \tag{34}$$

Leray-α model: $(C_1,C_2,C_3) = (C_4/2)\,(1,0,-1)$ and $(b_1,b_2,b_3) = (C_4/2)\,(1,1,0)$ expressed as

$$\frac{\partial\mathbf{v}}{\partial t} + (\mathbf{u}\cdot\nabla)\mathbf{v} + \nabla p = \nu\Delta\mathbf{v}. \tag{35}$$

Clark-α model: $(C_1,C_2,C_3) = (C_4/2)\,(-1,0,-3)$ and $(b_1,b_2,b_3) = (C_4/2)\,(0,1,0)$ expressed as

$$(1-\alpha^2\Delta)\left(\frac{\partial\mathbf{u}}{\partial t} + \mathbf{u}\cdot\nabla\mathbf{u} - \nu\Delta\mathbf{u}\right) + \nabla p = -\alpha^2\operatorname{div}(\nabla\mathbf{u}\cdot\nabla\mathbf{u}^T). \tag{36}$$

As a fourth choice, we shall alter the Leray-α model into the Bardina-α model, as

$$\frac{\partial\mathbf{v}}{\partial t} + (\mathbf{u}\cdot\nabla)\mathbf{u} + \nabla p = \nu\Delta\mathbf{v}. \tag{37}$$

These four special cases are chosen for their analytical regularity. The LANS-α model, the Clark-α model and the Bardina-α model (the first, third, and fourth choices) all provide analytical control of the L^2 norm of the velocity gradient, $\|\nabla\mathbf{u}\|$. This may be verified by taking the scalar product of the velocity $\mathbf{u}$ with each of these equations and integrating over the volume of flow, to find the energetics for homogeneous boundary conditions,

$$\frac{d}{dt}\int\frac{1}{2}|\mathbf{u}|^2 + \frac{1}{2}\alpha^2|\nabla\mathbf{u}|^2\,d^3x = -\nu\int|\nabla\mathbf{u}|^2d^3x - \nu\int\alpha^2|\Delta\mathbf{u}|^2\,d^3x. \tag{38}$$

This energy equation illustrates the reactive feature of these four models. The second term in the integrand on the left-hand side is the reactive term: kinetic energy (the first term) may be converted into enstrophy (the second term), not just into heat (the viscous terms on the right-hand side). Similarly, the Leray-α model controls the L^2 norm of the Laplacian of velocity, $\|\Delta\mathbf{u}\|$, as shown by taking its scalar product with the other velocity, $\mathbf{v}$. Thus, these models are reactive, as well as dissipative, and their energetic exchanges involve L^2 norms of velocity derivatives. Consequently, their solutions possess greater analytical regularity than solutions of the NS equations. We shall analyze the CC solutions for these four special choices among the nonlinear-reactive fluids as candidate turbulence models. The fourth model (Bardina-α) does not quite fit into the nonlinear-reactive stress tensor scenario of the first three models. Instead, the Bardina-α model arises naturally in the context of filtered NS equations for large eddy simulations. The interpretations of *solutions* of LES and RANS models are usually considered to be different. However, from the viewpoint of formal analysis of constitutive relations and elliptic instability, one cannot distinguish between LES and RANS equations. Therefore, with an apol-

ogy for our abuse of notation, and since the velocity **u** may be regarded as a filtered version of velocity **v** (filtered by inversion of the Helmholtz operator), we shall regard the four alpha models above as either RANS or LES models. Because only the first of these four models satisfies the conditions of MFI, we shall only consider this one, the LANS-α model, in a rotating frame.

IV. ROTATING CC SOLUTIONS OF THE LANS-α MODEL

We shall explain the CC solutions of the LANS-α model in full detail. The LANS-α model was derived by averaging over fluctuations along particle trajectories in Hamilton's variational principal for the Euler equations, then using Taylor's hypothesis for frozen-in fluctuations as a nonlinear turbulence closure in the framework of the Euler–Poincaré variational theory, before finally adding Navier–Stokes viscosity. See Ref. 7 and references therein for more details and subsequent developments. The LANS-α model closure equations for incompressible turbulence consist of the nonlinear-reactive fluid equations (29) and (30), subject to the relation $\alpha^2=C_0\ell^2C_4/2$ and coefficients $(b_1,b_2,b_3)=(C_4/2)(1,1,-1)$. The LANS-$\alpha$ equations can be expressed equivalently as in Eq. (34),

$$\frac{\partial\mathbf{v}}{\partial t}+(\mathbf{u}\cdot\nabla)\mathbf{v}+(\nabla\mathbf{u})^T\cdot\mathbf{v}+2\boldsymbol{\Omega}\times\mathbf{u}+\nabla\left(p-\frac{1}{2}|\mathbf{u}|^2-\frac{1}{2}\alpha^2|\nabla\mathbf{u}|^2\right)=\nu\Delta\mathbf{v}+\mathbb{F}, \tag{39}$$

with $\nabla\cdot\mathbf{u}=0$ and $\mathbf{v}=(1-\alpha^2\Delta)\mathbf{u}$. Here, ν is a turbulent eddy viscosity. Thus, the motion equation for the LANS-α model contains two velocities **u** and **v**. The transport velocity, **u**, is smoother than the transported velocity, **v**, by the inversion of the Helmholtz operator, $(1-\alpha^2\Delta)$.

In constructing CC solutions to the LANS-α equations (39), we again focus on base flows in the linear form $\mathbf{u}_0=\mathcal{S}(t)\cdot\mathbf{x}+\mathbf{U}(t)$ only. In this case, $\mathbf{v}_0=\mathbf{u}_0$ and the LANS-α CC equations for pressure and amplitude corresponding to the NS CC Eqs. (8) and (7) are given by

$$p_{12}-(\Upsilon-1)|\mathbf{a}|^2=0, \tag{40}$$

$$\frac{\mathrm{d}(\Upsilon\mathbf{a})}{\mathrm{d}t}+i(d_t\delta+\beta\mathbf{k}\cdot\mathbf{U})\Upsilon a+\Upsilon\mathcal{S}^T\cdot\mathbf{a}+\boldsymbol{\Pi}\times\mathbf{a}-(\beta\hat{p}_{11}-\alpha^2\beta^2\mathbf{a}\cdot\mathcal{S}\cdot\mathbf{k})\mathbf{k}=-\Upsilon E_\omega|\mathbf{k}|^2\mathbf{a}. \tag{41}$$

Equations (6) and (9) for the CC solution properties of frozen-in phase and transverse amplitude, respectively, remain unchanged for the LANS-α model. Here, the LANS-α CC variables are defined the same as for the classical NS CC solutions, and the quantity $\Upsilon(t)$ is given by

$$\Upsilon(t)=1+\alpha^2\beta^2|\mathbf{k}(t)|^2. \tag{42}$$

Without loss of generality, we may again set $\mathrm{d}\delta/\mathrm{d}t+\beta\mathbf{k}\cdot\mathbf{U}=0$ for the kinematic phase condition, assume that $\mathbf{a}(t)$ is a real-valued function, and obtain Eq. (10) for $\mathbf{k}(t)$. We may also solve the pressure as before to obtain

$$\tilde{P}=\frac{1}{|\mathbf{k}|^2}\{\Upsilon\mathbf{k}\cdot(\mathcal{S}+\mathcal{S}^T)\cdot\mathbf{a}+\boldsymbol{\Pi}\times\mathbf{a}\cdot\mathbf{k}\}, \tag{43}$$

where $\tilde{P}$ is the coefficient of **k** in Eq. (41). As in the NS case, viscosity may be transformed out of the problem by considering the same change of variables as in Eq. (11). Note that the term $i(d_t\delta+\beta\mathbf{k}\cdot\mathbf{U})$ was incorrectly placed in the eikonal equation (6) in Ref. 8. The difference, however, is trivial and does not affect the results of that investigation.

Insight into the dynamics of the LANS-α CC problem can be gained by examining Eq. (41) in the asymptotic regimes $\Gamma\ll1$ and $\Gamma\gg1$, where for brevity of notation we introduce $\Gamma=\Upsilon-1$. We shall assume that $|\mathbf{k}|^2$ remains bounded and never vanishes. In these extreme parameter regimes, Eq. (41) becomes

$$\frac{\mathrm{d}\mathbf{a}}{\mathrm{d}t}+\mathcal{S}^T\cdot\mathbf{a}=-E_\omega|\mathbf{k}|^2\mathbf{a}-\boldsymbol{\Pi}\times\mathbf{a}+\frac{1}{|\mathbf{k}|^2}(\mathbf{k}\cdot(\mathcal{S}+\mathcal{S}^T)\cdot\mathbf{a}+\boldsymbol{\Pi}\times\mathbf{a}\cdot\mathbf{k})\mathbf{k}+\Gamma\left(\boldsymbol{\Pi}\times\mathbf{a}+\frac{1}{|\mathbf{k}|^2}\{2(\mathbf{k}\cdot\mathcal{S}\cdot\mathbf{k})\mathbf{a}-(\boldsymbol{\Pi}\times\mathbf{a}\cdot\mathbf{k})\mathbf{k}\}\right)+O(\Gamma^2),\quad \Gamma\ll1, \tag{44}$$

$$\frac{\mathrm{d}\mathbf{a}}{\mathrm{d}t}+\mathcal{S}^T\cdot\mathbf{a}=-E_\omega|\mathbf{k}|^2\mathbf{a}+\frac{2}{|\mathbf{k}|^2}\{(\mathbf{k}\cdot\mathcal{S}\cdot\mathbf{k})\mathbf{a}-(\mathbf{k}\cdot(\mathcal{S}+\mathcal{S}^T)\cdot\mathbf{a})\mathbf{k}\}+O\left(\frac{1}{\Gamma}\right),\quad \Gamma\gg1. \tag{45}$$

These equations preserve the wave transversality condition $\mathbf{a}\cdot\mathbf{k}=0$ to all orders. However, as we shall explain, care should be taken in interpreting these LANS-α CC equations when $\nu>0$, since the Ekman number E_ω contains a factor of β^2. The parameter α is interpreted as the nondimensional turbulence correlation length for Lagrangian fluid trajectories in the LANS-α model and $\alpha<1$ is typically regarded as a small, fixed number. In this case, the two limits $\Gamma\ll1$ and $\Gamma\gg1$ correspond to low and high wave numbers, respectively. The $O(1)$ term in Eq. (44) for low wave numbers is exactly Eq. (7) for NS. This is not unexpected, since LANS-α reduces to NS for $\alpha=0$. We see in Eq. (44) that the amplitude **a** decays exponentially with viscosity, while it stretches with the base shear, and rotates with the vorticity of the undisturbed system. When the limit $\Gamma\ll1$ corresponds to fixed α and low β, the evolution is essentially inviscid. In the opposite limit, for $\Gamma\gg1$, the terms of order $O(1/\Gamma)$, and smaller, are independent of E_ω. In this limit, the amplitude to leading order still decays with viscosity and stretches with the base shear as in the low wave-number case, but the effects of rotation with the total vorticity $\boldsymbol{\Pi}$ are higher order. In particular, when $\Gamma\gg1$ corresponds to fixed α and $\beta\to\infty$, the viscous term on the right-hand side of Eq. (45) is $O(\beta^2)$, from which we conclude that the amplitude decays exponentially with viscosity to leading order.

A. Inviscid LANS-α CC solutions

Circular inviscid LANS-α flowlines: For the LANS-α model, when the flowlines are circular and the flow is inviscid, then $\gamma=0$ and $E_\omega=0$. In this case, the elliptic instability problem can again be solved analytically. Since $|\mathbf{k}|=1$, the quantity Υ in Eq. (42) becomes constant, which we denote by $\Upsilon_0=1+\alpha^2\beta^2$. Equations (15)–(17) provide three linearly independent solutions to Eq. (41) when $\xi(t)=2t(1+\Omega)\cos\theta/\Upsilon_0$. Once again, we may construct the monodromy matrix explicitly, and the eigenvalues are again $\rho_{1,2}=\exp\{\pm i\xi(2\pi)\}$, $\rho_3=1$. By the same arguments as before, the critical stability points are now determined by

$$\cos\theta=\pm\frac{n\Upsilon_0}{2(1+\Omega)},\quad n=1,2,3,\ldots. \tag{46}$$

Since $|\cos\theta|\leqslant 1$, it follows that there are no critical stability points for

$$-\tfrac{1}{2}\Upsilon_0<\Omega+1<\tfrac{1}{2}\Upsilon_0. \tag{47}$$

The average maximum growth rate for small values of eccentricity $\gamma\ll 1$ may again be calculated as

$$\overline{\sigma_g}=\frac{(2+\Upsilon_0)^2}{16}\gamma\times\frac{(2+\Upsilon_0+2\Omega)^2}{(2+\Upsilon_0)^2(1+\Omega)^2}+O(\gamma^2), \tag{48}$$

which is valid for $\Upsilon_0\leqslant 2$ and Ω outside the range in Eq. (47).

Elliptical LANS-α flowlines: For nonzero values of eccentricity γ, the solution to Eq. (41) for the LANS-α wave amplitude must be simulated numerically. We find that for $\Omega\neq -1$ and $\Upsilon_0>1$, there exists a principal instability region in the $(\gamma,\cos\theta)$ parameter plane; see Figs. 3 and 4. For nonzero eccentricity γ, and for Ω satisfying Eq. (47), we find a band of eccentricities for which the amplitude **a** remains bounded. Thus the flow is stable in this band. In particular, the entire $(\gamma,\cos\theta)$ parameter plane is stable for $\Omega=-1$. For Ω outside the range in Eq. (47), we also find a large number of fingers which lie above (respectively, below) the principal instability region for $\cos\theta>0$ (respectively, $\cos\theta<0$). The fingers are exactly those we saw in the NS equations. However, for $\Upsilon_0>1$ these fingers become more significant and their widths increase. The growth rates associated with the fingers also increase. In fact, the maximum growth rate over the entire parameter plane increases to a maximum value of $\overline{\sigma_g}=\gamma$ at $\cos\theta=1$, i.e., at $\Upsilon_0=2(1+\Omega)$. As Υ_0 exceeds this threshhold, a stable band of eccentricities appears and the maximum growth rate begins to decrease. See Fig. 3. Thus, the wave number at which the growth rate attains a maximum is not only a function of the turbulence correlation length, α, but it also depends on the inverse Rossby number, Ω. For the inviscid case, the results in the limits $\alpha^2\beta^2\ll 1$ and $\alpha^2\beta^2\gg 1$ are independent of whether α is fixed and $\beta\to\infty$, or vice versa.

Remark: We observed during numerical simulations that the change of the instability domain for $0\leqslant\alpha^2\beta^2<\infty$ with $\Omega=0$ is extraordinarily similar to that for $-1\leqslant\Omega\leqslant 0$ with $\alpha^2\beta^2=0$. In fact, the two different cases will have the same principal critical angle when

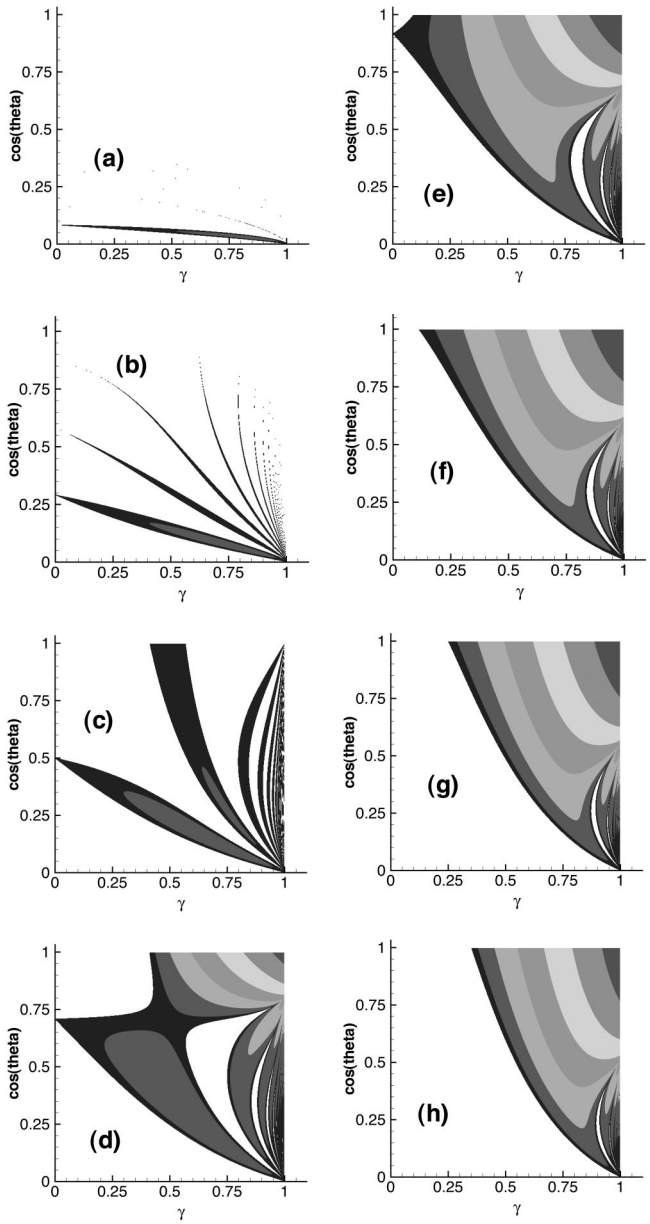

FIG. 3. Instability domains for CC solutions in LANS-α model for $E_\omega=0$, $\Omega=5$ and various values of $\alpha^2\beta^2$: (a) 0.0, (b) 2.5, (c) 5.0, (d) 7.5, (e) 10.0, (f) 12.5, (g) 15, (h) 17.5. The white background represents regions for which $\sigma_g<10^{-10}$. As $\alpha^2\beta^2$ increases, the angle of critical stability shifts according to Eq. (46). The nonprincipal fingers correspond to critical angles with $n>1$. The parameter $\alpha^2\beta^2$ shifts the angle of critical stability towards $\cos\theta=1$ while increasing the maximum growth rate. As $\alpha^2\beta^2$ exceeds $1+2\Omega$ (f), a stable band of eccentricities appears and the maximum growth rate decreases.

$$\Omega=\frac{-\alpha^2\beta^2}{1+\alpha^2\beta^2}. \tag{49}$$

Although the two instability domains in Ω and $\alpha^2\beta^2$ do not overlap exactly, numerical simulations show that where they do overlap, the difference in the growth rates is small. In particular, the relative difference of the individual maximum growth rates, which occur at $\cos\theta=1$, $\gamma=1$ when $\alpha^2\beta^2\geqslant 1$ (or equivalently, $-1<\Omega<-\frac{1}{2}$), is less that 1%. Since Eq. (49) can be rewritten as $\alpha^2\beta^2=-\Omega/(1+\Omega)$, valid for -1

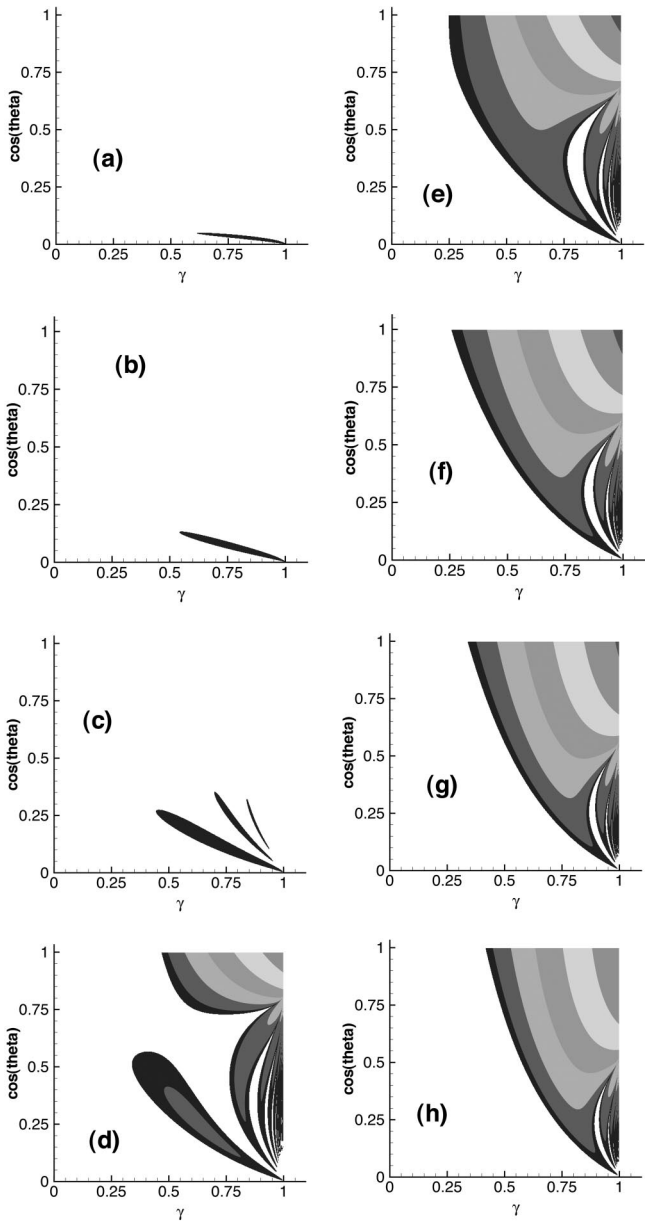

FIG. 4. Instability domain for CC solutions in LANS-α for $E_\omega=0.1$, $\Omega=5$ and various values of $\alpha^2\beta^2$ (compare with Fig. 3): (a) 0.0, (b) 2.5, (c) 5.0, (d) 7.5, (e) 10.0, (f) 12.5, (g) 15.0, (h) 17.5. The white background represents regions for which $\sigma_g<10^{-10}$. The results are similar to those in Fig. 3 with a stable band of eccentricities introduced by viscosity. Of particular interest is the introduction of an instability finger emanating from $\cos\theta=1$, $\gamma=1$ (d) and merging with the principal finger (e).

$\leqslant\Omega\leqslant 0$, we conclude that the effect of α in the LANS-α model on elliptic instability is essentially equivalent to counter rotation of the coordinate system.

B. Viscous LANS-α CC solutions

Landman and Saffman[13] extended Bayly's elliptic instability analysis to add viscous effects. They found that viscosity decreases the growth rate and introduces a high wave number cutoff in the $(\gamma,\cos\theta)$ plane. For $\Upsilon_0>1$ in the LANS-α model, viscosity again introduces a high wave number cutoff. However, for fixed E_ω, the LANS-α model destabilizes some (but not all) of the eccentricities as $\Upsilon_0=1+\alpha^2\beta^2$ increases from unity to two while shifting the critical stability angle towards $\cos\theta=1$. Figure 5 shows the neutral stability surface for the nonrotating case. In particular, the entire $(\gamma,\cos\theta)$ parameter plane can be stable for fixed large values of E_ω and $\Upsilon_0=1$, then destabilize as Υ_0 increases to two, and then stabilize again [Fig. 5(c)]. To emphasize the effects of fixed α and various β as described by the asymptotics, Fig. 6 shows a representative surface for various values of $\nu/|\omega|$. Finally, in Fig. 7, we show the growth rates maximized over the $(\cos\theta,\gamma)$ plane.

Rotation intensifies the effects of Υ_0, and viscosity dampens out many of the insignificant fingers. In fact, the physically insignificant fingers are removed by viscosity from the contour plots, and we are left with only the main region. See Fig. 4.

V. CC SOLUTIONS IN FOUR TURBULENCE MODELS, IN THE ABSENCE OF ROTATION

The field of large eddy simulation (LES) models is driven by the desire to simulate reliably the motion of the large scales in turbulent flow, without completely simulating the smaller scales. A common approach is to introduce a filter operation $L(\cdot)$ and to examine the evolution of a filtered velocity field $\mathbf{u}$ which corresponds to an exact velocity field $\mathbf{v}$ by the relationship $\mathbf{u}=L(\mathbf{v})$. Introducing filtering causes the effects of length scales smaller than the width of the filter to become negligible. Focusing on nonrotating coordinate systems, the resulting LES equation for $\mathbf{u}$ is

$$\partial_t\mathbf{u}+\mathbf{u}\cdot\nabla\mathbf{u}-\nu\Delta\mathbf{u}+\nabla\tilde{p}-\tilde{\mathbb{F}}-\nu\Delta\mathbf{u}=-\operatorname{div}\tau(\mathbf{u}), \tag{50}$$

where $\operatorname{div}\mathbf{u}=0$. The variables $\tilde{p}$ and $\tilde{\mathbb{F}}$ are the filtered pressure and body forces, respectively, and $\tau(\mathbf{u})=L(\mathbf{vv})-\mathbf{uu}$ is the LES closure for the stress tensor. Just as in RANS modeling, the bulk of the work in LES modeling focuses on deriving a form for τ based on physical assumptions, e.g., symmetry, material frame indifference, etc. We apologize again for conflating these two approaches in a single treatment. However, from the viewpoint of formal analysis of CC solutions for nonlinear-reactive fluids, based on their constitutive relations, one cannot distinguish between LES and RANS.

A. LANS-α and other nonlinear-reactive-fluid models of turbulence

As we discussed earlier, the LANS-α model in Eq. (39) may be expressed as

$$(1-\alpha^2\Delta)(\partial_t\mathbf{u}+\mathbf{u}\cdot\nabla\mathbf{u}-\nu\Delta\mathbf{u})+\nabla p-\mathbb{F}=-\alpha^2\operatorname{div}\tau \tag{51}$$

together with $\operatorname{div}\mathbf{u}=0$, where $\operatorname{div}\tau$ is the right-hand side of Eq. (30). Comparing Eq. (51) with Eq. (50), we see that $(1-\alpha^2\Delta)^{-1}\operatorname{div}\tau$ is equivalent to the divergence of a filtered stress tensor, for which the filtering is performed by inversion of the Helmholtz operator $(1-\alpha^2\Delta)$. We emphasize that the filtering in Eq. (30) is not a modeling choice (as is the norm in LES modeling); rather, it is a reformulation of

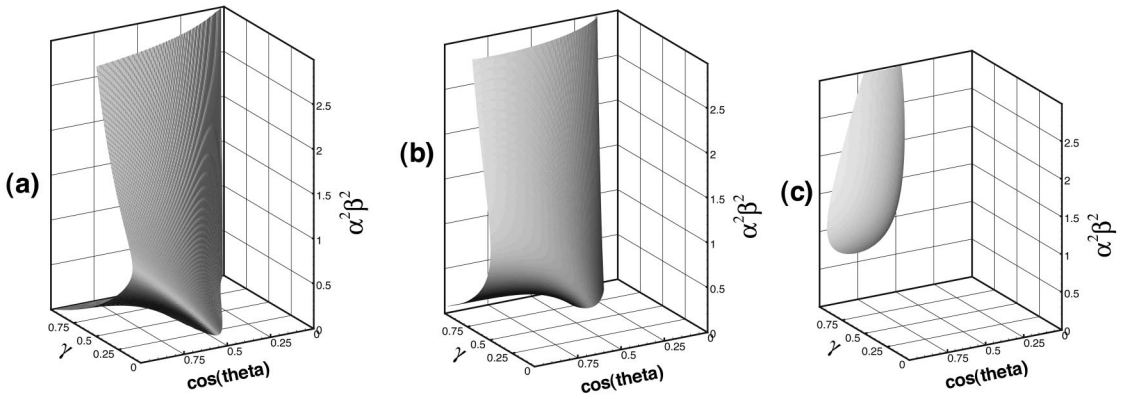

FIG. 5. Approximation of the neutral stability surface (i.e., $\sigma_g = 0.01$) for CC solutions in LANS-α for $\Omega = 0$, fixed $\beta = 1.0$, and various values of E_ω: (a) 0.1, (b) 0.5, (c) 1.0.

the LANS-α model. We shall search for CC solutions to Eq. (51) in full generality and will omit terms *a posteriori* to investigate the various models.

CC solutions for the nonlinear-reactive fluids: Let us define $\mathbf{u} = \mathbf{u}_0 + \mathbf{u}_1$, $p = p_0 + p_1$, where $\mathbf{u}_0 = \mathcal{S}(t)\cdot\mathbf{x} + \mathbf{U}(t)$ is an exact solution to Eq. (51) and p_0 is the corresponding pressure as before, and $\{\mathbf{u}_1, p_1\}$ are as in Eq. (1). Again incompressibility yields wave transversality, as expressed in Eq. (9). The resulting equations for the amplitude $\mathbf{a}$, the phase ψ, and the pressure terms are obtained as before by collecting on terms linear and constant in $\mathbf{x}$:

$$p_{12} - b_3\alpha^2\beta^2|\mathbf{a}|^2|\mathbf{k}|^2 = 0, \tag{52}$$

$$\partial_t(\mathbf{k}\cdot\mathbf{x}) + \mathbf{k}\cdot\mathcal{S}\cdot\mathbf{x} = 0, \tag{53}$$

$$\begin{aligned}\Upsilon\frac{d\mathbf{a}}{dt} + i\Upsilon(d_t\delta + \beta\mathbf{U}\cdot\mathbf{k})\mathbf{a} - 2i\alpha^2\beta^2((d_t\mathbf{k} + \mathbf{k}\cdot\mathcal{S})\cdot\mathbf{k})\mathbf{a}\\ + (\Upsilon - b_1(\Upsilon-1))\mathcal{S}\cdot\mathbf{a} - b_3(\Upsilon-1)\mathcal{S}^T\cdot\mathbf{a} + E_\omega|\mathbf{k}|^2\Upsilon\mathbf{a}\\ - (\beta p_{11} + b_3\alpha^2\beta^2(\mathbf{a}\cdot\mathcal{S}\cdot\mathbf{k}))\mathbf{k}\\ = \alpha^2\beta^2(b_1+b_2)(\mathbf{k}\cdot\mathcal{S}\cdot\mathbf{k})\mathbf{a}.\end{aligned} \tag{54}$$

Here, we are keeping track of the contributions of various terms in the stress tensor, thereby allowing us to examine all the models simultaneously. As in the NS case, we set $d\delta/dt + \beta\mathbf{k}\cdot\mathbf{U} = 0$. We take the gradient of Eq. (53) to obtain Eq. (10) for the evolution of $\mathbf{k}$. Then the third term in Eq. (54) vanishes exactly, and we assume that $\mathbf{a}(t)$ is a real-valued function. Again, we remove the effects of viscosity by an integrating factor. Finally, we use the identity $d\Upsilon/dt = -2\alpha^2\beta^2\mathbf{k}\cdot\mathcal{S}\cdot\mathbf{k}$ to obtain

$$\begin{aligned}\frac{d(\Upsilon\mathbf{a})}{dt} + (\Upsilon - b_1(\Upsilon-1))\mathcal{S}\cdot\mathbf{a} - b_3(\Upsilon-1)\mathcal{S}^T\cdot\mathbf{a}\\ + E_\omega|\mathbf{k}|^2\Upsilon\mathbf{a} - \tilde{P}\mathbf{k}\\ = \alpha^2\beta^2(b_1+b_2-2)(\mathbf{k}\cdot\mathcal{S}\cdot\mathbf{k})\mathbf{a},\end{aligned} \tag{55}$$

where $\tilde{P}$ is the coefficient of $\mathbf{k}$ in Eq. (54)

1. LANS-α

The LANS-α model corresponds to $(b_1, b_2, b_3) = (1, 1, -1)$ in Eqs. (52)–(54). These are the equations we examined in Sec. IV.

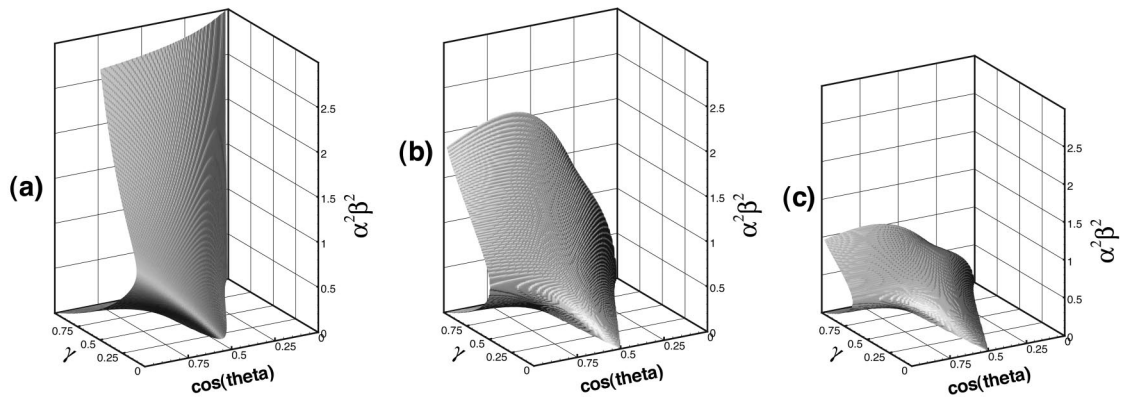

FIG. 6. Approximation of the neutral stability surface (i.e., $\sigma_g = 0.01$) for CC solutions in LANS-α for $\Omega = 0$, fixed $\alpha = 1.0$, and various values of $\nu/|\omega|$: (a) 0.1, (b) 0.5, (c) 1.0. Notice that the flow behaves inviscidly for $\alpha^2\beta^2 \ll 1$ and decays exponentially fast as $\alpha^2\beta^2$ increases as predicted by the asymptotics.

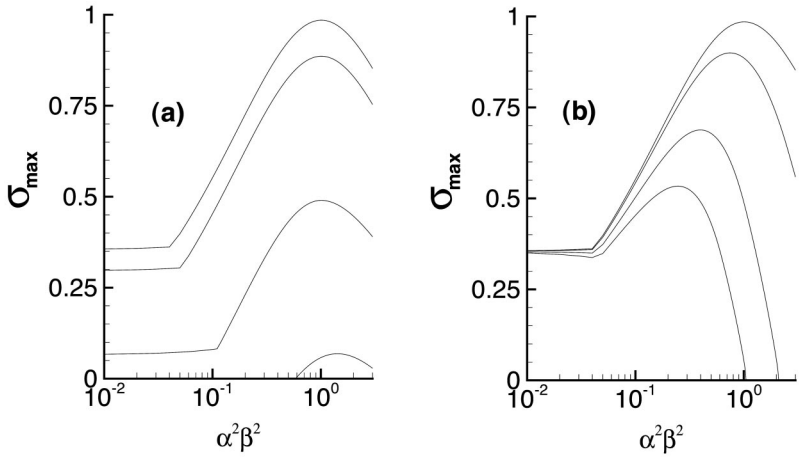

FIG. 7. The maximum growth rates in LANS-α for different values of $\nu/|\omega|$ and $\Omega=0.0$. In each picture, the values of $\nu/|\omega|$ are, from top to bottom, 0, 0.1, 0.5, and 1.0. (a) corresponds to fixed $\beta=1.0$ and various α, and (b) to fixed $\alpha=1.0$ and various β.

2. Leray-α

Leray[25] introduced a class of regularized NS equations, which for Helmholtz-inversion filtering we call the Leray-α model. These equations were introduced not as a turbulence closure model, but rather as a deformation of the NS equations, for which Leray was able to show global existence and uniqueness of solutions. The Leray-α model is similar to the LANS-α model and may be written as

$$\partial_t \mathbf{v}+\mathbf{u}\cdot\nabla\mathbf{v}+\nabla p=\nu\Delta\mathbf{v}, \tag{56}$$

with pressure determined by preservation of $\mathrm{div}\,\mathbf{u}=0$ and $\mathbf{v}=(1-\alpha^2\Delta)\mathbf{u}$. The Leray-$\alpha$ model corresponds to $(b_1,b_2,b_3)=(1,1,0)$ in Eqs. (52)–(54). The equations of motion for the Leray-α CC solutions are Eqs. (9), (10), and

$$p_{12}=0, \tag{57}$$

$$\frac{\mathrm{d}(\Upsilon\mathbf{a})}{\mathrm{d}t}+\mathcal{S}\cdot\mathbf{a}-\beta p_{11}\mathbf{k}+E_\omega|\mathbf{k}|^2\Upsilon\mathbf{a}=\mathbf{0}. \tag{58}$$

The specific case of elliptic instability for the Leray-α model is similar to the CC analysis for the NS equations. The wave vector $\mathbf{k}$ is given in Eq. (14) with $\chi(t)=t\sqrt{1-\gamma^2}$. For $\gamma=0$, in the case of circular flowlines, the Leray-α solutions for the wave amplitude $\mathbf{a}$ arise as in Eqs. (15)–(17), except with $\xi(t)=t(1+\Upsilon_0)\cos\theta/\Upsilon_0$. For elliptical flowlines with nonzero γ, we again may use Floquet theory.

Figure 8 shows the critical stability surface for elliptic instability in the Leray-α model. The effects are drastically different from those of the LANS-α model. The angle of critical stability shifts according to the formula $\cos\theta=\Upsilon_0/(1+\Upsilon_0)$. Since this quantity is always less than unity in magnitude, no stable band of eccentricities ever appears. Furthermore, the maximum growth rate has an average value calculated as before of $\overline{\sigma_g}=(1+2\Upsilon_0)^2\gamma/\{4\Upsilon_0(1+\Upsilon_0)^2\}$ to leading order in $\gamma\ll 1$ for all values of $\alpha^2\beta^2$. Thus, as $\alpha^2\beta^2$ increases from zero, the maximum growth rate *decreases* as a function of $\alpha^2\beta^2$. However, the parameter $\alpha^2\beta^2$ does not introduce a stable band of eccentric Leray-α flows.

3. Helmholtz-filtered Clark-α model

The Helmholtz-filtered Clark-α model[26–28] corresponds to $(b_1,b_2,b_3)=(0,1,0)$ in Eqs. (52)–(54). The resulting CC equations for the elliptic instability dynamics of the linear base flow $\mathbf{u}_0=\mathcal{S}\cdot\mathbf{x}+\mathbf{U}$ are Eqs. (8), (6), (9), plus

$$\Upsilon\frac{\mathrm{d}\mathbf{a}}{\mathrm{d}t}+\Upsilon\mathcal{S}\cdot\mathbf{a}-\beta p_{11}\mathbf{k}+E_\omega|\mathbf{k}|^2\Upsilon\mathbf{a}-\alpha^2\beta^2(\mathbf{k}\cdot\mathcal{S}\cdot\mathbf{k})\mathbf{a}=\mathbf{0}. \tag{59}$$

Note that the integrating factor

$$\mathbf{a}(t)=\hat{\mathbf{a}}(t)\exp\left(\int_0^t\frac{\alpha^2\beta^2\mathbf{k}(\hat{t})\cdot\mathcal{S}(\hat{t})\cdot\mathbf{k}(\hat{t})}{\Upsilon(\hat{t})}d\hat{t}\right) \tag{60}$$

will reduce the problem to that for the Euler equations. Thus, the growth rate for the Clark-α model is modified by

$$\sigma_{g,\mathrm{Clark}}=\sigma_{g,\mathrm{Euler}}+\frac{1}{\tau_p}\int_0^{\tau_p}\frac{\alpha^2\beta^2\mathbf{k}(\hat{t})\cdot\mathcal{S}(\hat{t})\cdot\mathbf{k}(\hat{t})}{\Upsilon(\hat{t})}d\hat{t}.$$

For the case of elliptic instability for which $\mathcal{S}(t)$ is given in Eq. (2), the wave vector $\mathbf{k}(t)$ is given in Eq. (10) and the

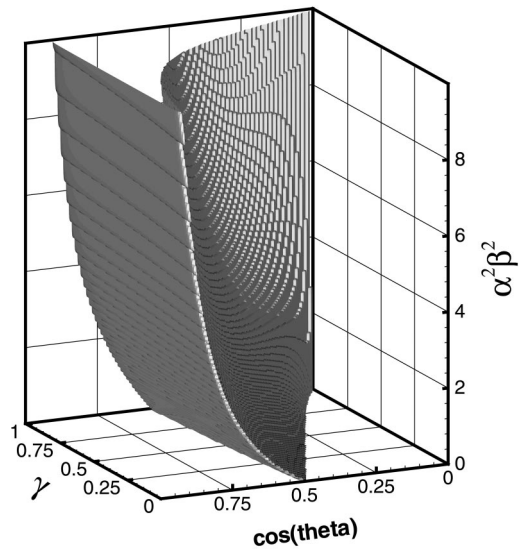

FIG. 8. Critical stability surface for elliptic instability in the Leray-α model for $0\leqslant\alpha^2\beta^2\leqslant 10$, $E_\omega=0$. Again, Fig. 1 corresponds to the slice $\alpha^2\beta^2=0$. The critical angle shifts as predicted, though always touches the slice $\gamma=0$.

period is $\tau_p = 2\pi/\sqrt{1-\gamma^2}$, the above integral vanishes exactly. Consequently, the Helmholtz-filtered Clark-α model *preserves exactly the NS elliptic instability*.

B. Bardina-α model

The Bardina-α model[29] is similar to those above, but it does not arise as a choice in Eq. (30) for the stress tensor. The motion equation for the Bardina-α model is

$$\partial_t \mathbf{v} + \mathbf{u}\cdot\nabla\mathbf{u} + \nabla p = \nu\Delta\mathbf{v}, \tag{61}$$

with pressure determined by preservation of $\operatorname{div}\mathbf{v}=0$ and $\mathbf{v}=(1-\alpha^2\Delta)\mathbf{u}$. This model still uses the inverse Helmholtz filter, albeit with a different stress tensor. As was the case for all previous models, the elliptical columnar flow is an exact solution subject to the same conditions. We construct a CC solution by adding the Kelvin traveling wave to the column and collecting on terms linear and constant in $\mathbf{x}$. The resulting equations of motion for elliptic instability are Eqs. (8), (9), plus

$$\Upsilon\,\partial_t(\mathbf{k}\cdot\mathbf{x}) + \mathbf{k}\cdot\mathcal{S}\cdot\mathbf{x} = \mathbf{0}, \tag{62}$$

$$\partial_t(\Upsilon\,\mathbf{a}) + i\,\mathbf{a}(\Upsilon\,\partial_t\delta + \beta\mathbf{k}\cdot\mathbf{u}) + \mathcal{S}\cdot\mathbf{a} - p_{11}\mathbf{k} + \nu|\mathbf{k}|^2\Upsilon\,\mathbf{a} = \mathbf{0}. \tag{63}$$

The first observation is that Υ does not factor out of the equation for the wave vector $\mathbf{k}$ as it did before. This is due to the fact that the model's nonlinearity is of the form $\mathbf{u}\cdot\nabla\mathbf{u}$, and not $\mathbf{u}\cdot\nabla\mathbf{v}$ as in the previous models. This means that, upon taking the gradient of Eq. (62), we obtain the following *nonlinear* equation for the evolution of $\mathbf{k}$:

$$\frac{d\mathbf{k}}{dt} + \frac{(\nabla\mathbf{u}_0)^T\cdot\mathbf{k}}{1+\alpha^2\beta^2|\mathbf{k}|^2} = \mathbf{0}. \tag{64}$$

That is, the wave vector $\mathbf{k}(t)$ is no longer frozen into the fluid. We shall analyze the specific case of elliptic instability. Numerical simulations indicate that the components of $\mathbf{k}$ are periodic. Upon guessing a solution in the form of Eq. (14), we find that $\chi(t)$ is the solution to the transcendental equation

$$\left(1+\alpha^2\cos^2\theta + \frac{\alpha^2\sin^2\theta}{1+\gamma}\right)\chi(t) + \frac{\alpha^2\gamma\sin^2\theta}{2(1+\gamma)}\sin(2\chi(t)) = t\sqrt{1-\gamma^2}. \tag{65}$$

For the case $\gamma=0$, we have that $\chi(t)=t/(1+\alpha^2)$ exactly. For small nonzero eccentricity of the flowlines, $\gamma\ll 1$, we may neglect the nonlinear term in $\chi(t)$ to find

$$\chi(t) \approx \frac{t\sqrt{1-\gamma^2}}{1+\alpha^2\cos^2\theta + \alpha^2\sin^2\theta/(1+\gamma)}. \tag{66}$$

Although this choice of $\chi(t)$ is not an accurate approximation, numerical simulations show that it is sufficient to determine the periodicity of the wave vector $\mathbf{k}$ for all parameter regimes. Consequently, the wave amplitude $\mathbf{a}$ again satisfies a Floquet problem, whose period is determined by Eq. (66). As before, we assume that $\mathbf{a}$ is a real-valued function upon setting $\Upsilon\,\mathbf{d}\delta/dt + \beta\mathbf{k}\cdot\mathbf{U} = 0$.

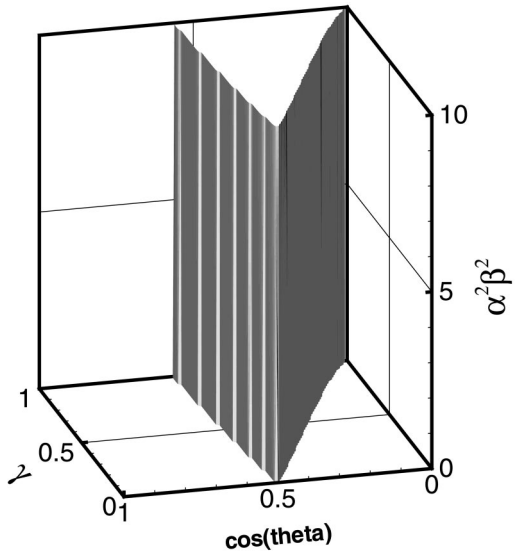

FIG. 9. Critical stability surface for elliptic instability in the Bardina-α model for $0 \leqslant \alpha^2\beta^2 \leqslant 10$, $E_\omega = 0$. Again, Fig. 1 corresponds to the slice $\alpha^2\beta^2 = 0$.

Circular Bardina-α flowlines: The case $\gamma=0$ for the Bardina-α model can be simplified by considering a change of time variable $t_n = t/(1+\alpha^2)$. In this new variable, the equations recover exactly those for the classical Euler case. Thus, the angle of critical stability is again $\cos\theta = 1/2$, and the average maximum growth rate, under appropriate scalings, is $\overline{\sigma_g} = 9\gamma/\{16\Upsilon_0\}$. Thus, the effect of the Bardina model on elliptic instability is to *reduce* the average maximum growth rate for all values of α but not shift the angle of critical stability. See Fig. 9.

VI. DISCUSSION

We have examined the CC class of exact nonlinear solutions for several recently introduced turbulence closure models that appear in the framework of nonlinear-reactive fluid dynamics. We find that all these models preserve the existence of elliptic instability. This is a desired property of any turbulence model—it should at least preserve the classic NS instabilities. We emphasize that elliptic instability is generated by the nonlinear term in the NS equations, via parametric resonance mediated by vortex stretching. Thus, the choice of the nonlinearity plays a crucial role in elliptic instability. In the models we have examined here, the effect of the nonlinearity choice on the CC class of solutions determines the presence of the function $\Upsilon(t)$ in the amplitude equation (54). For example, Υ appears linearly in the Clark-α model and factors out of the equation, and thus elliptic instability is unaltered in this model. In contrast, the presence of $\Upsilon(t)$ in the Bardina-α model leads to a nonlinear equation for the wave vector $\mathbf{k}$. Since the term quadratic in the disturbance $\mathbf{u}_1\cdot\nabla\,\mathbf{u}_1$ vanishes as a result of transversality, $\mathbf{a}\cdot\mathbf{k}=0$, the instability is a result of wave-mean-flow interaction, rather than wave–wave interaction. Thus, elliptic instability is complementary to the triad resonance mechanism, which results from nonlinear wave–wave interaction generated by the quadratic disturbance term.

TABLE I. All of the nonlinear-reactive-fluid models of turbulence preserve the classic CC solutions for base flows of the form $\mathbf{u}_0=\mathcal{S}\cdot\mathbf{x}+\mathbf{U}$. The second column lists the angle of critical stability for the linear flows of the form in Eq. (2) for $\Omega=0$, where for brevity $\Upsilon_0=1+\alpha^2\beta^2$. The third column lists the average maximum growth rate to leading order in the eccentricity γ. Note that in all the models, the values for NS are regained by setting $\alpha^2\beta^2=0$.

Model	Principal critical angle	Maximum growth rate
NS	$\cos\theta=1/2$	$\overline{\sigma_g}=9\gamma/16$
LANS-α	$\cos\theta=\Upsilon_0/2$	$\overline{\sigma_g}=(2+\Upsilon_0)^2\gamma/16$
Leray-α	$\cos\theta=\Upsilon_0/(\Upsilon_0+1)$	$\overline{\sigma_g}=(2\Upsilon_0+1)^2\gamma/(4\Upsilon_0(\Upsilon_0+1)^2)$
Clark-α	$\cos\theta=1/2$	$\overline{\sigma_g}=9\gamma/16$
Bardina-α	$\cos\theta=1/2$	$\overline{\sigma_g}=9\gamma/(16\Upsilon_0)$

Our main conclusion is that these models alter the NS structure of the CC solutions. Detailed results for (i) the critical instability angle, and (ii) the average maximum growth rate for the various turbulence closure models are summarized and compared in Table I and Fig. 10. Perhaps surprisingly, the Bardina-α model is identified in Table I of comparisons as preserving more features of the CC solutions for the NS equation than any of the other models. The model has the salient features that it decreases the growth rate for high wave numbers as is expected of LES models without altering the underlying physics, that is, it does not alter the critical angle of stability. Bardina-α is a new model, whose analytical properties, for example, will be considered in detail elsewhere.

Cambon *et al.*[30] examined from a statistical viewpoint the effects of a specific model on elliptic instability, hyperbolic instability, and the stability of Taylor–Green vortices. Our work complements their work in presenting a combination analytic and numerical results for a variety of turbulence models whose regularization is based on Helmholtz-inversion filtering. See Geurts and Holm[31] for an extension of other classes of filters of this regularization approach for turbulence modeling.

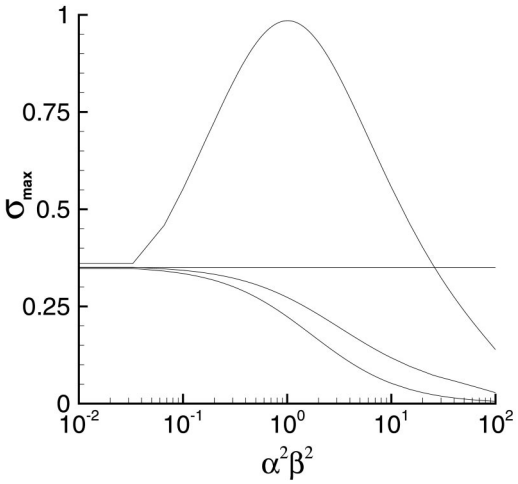

FIG. 10. The growth rates maximized over the $(\cos\theta,\gamma)$ plane as functions of $\alpha^2\beta^2$ for $E_\omega=0$. From top to bottom, the curves are for the LANS-α model, the NS equations and the Clark model (both are the flat line), the Leray-α model, and the Bardina-α model. The curves agree with the theoretical predictions. The curve for the LANS-α model will converge to zero in the limit $\alpha^2\beta^2\to\infty$.

ACKNOWLEDGMENTS

We thank A. Lifschitz-Lipton for sparking our original interest in CC solutions. One of the authors (B.F.) thanks the Theoretical Division of the Los Alamos National Laboratory for its continued hospitality.

APPENDIX: VERIFICATION OF THE BARDINA MODEL

The work in Sec. V B relied on approximating the period of $\mathbf{k}(t)$ correctly. As a check of this approximation, we use the quasiperiodic extension of Floquet theory as demonstrated in Ref. 32. We use the incompressibility condition Eq. (9) to eliminate a variable, say a_3, and rewrite the system in Eq. (63) as $d_t\mathbf{a}_\perp=\mathcal{B}\mathbf{a}_\perp$, where $\mathbf{a}_\perp=(a_1\ a_2)^T$. By using the Prüfer transformation

$$a_1(t)=e^{d(t)}\sin[c(t)],\quad a_2(t)=e^{d(t)}\cos[c(t)],\qquad \text{(A1)}$$

we rewrite the ODE in the new variables $c(t)$ and $d(t)$. The quantities

$$I=\lim_{t\to\infty}[d(t)/t],\quad W=\lim_{t\to\infty}\lim[c(t)],\qquad \text{(A2)}$$

called the growth rate and winding number, respectively, can be reliabilty simulated numerically by long time computations (say $t=1000$). The growth rate I is equivalent to the Lyapunov growth rate generated by Floquet theory. We compute these quantities on a coarse grid to verify that the Floquet theory analysis given above is accurate. Although the period of $\mathbf{k}$ may be only approximate, a numerical investigation using Floquet theory requires significantly less computing time than the present quasiperiodic theory.

[1]Precisely the equations for elliptic instability emerge, when the critical layer assumption (frozen-in phase) is substituted into the equations of Gjaja and Holm [I. Gjaja and D.D. Holm, "Self-consistent Hamiltonian dynamics of wave mean-flow interaction for a rotating stratified incompressible fluid," Physica D **98**, 343 (1996)] for self-consistent Lagrangian-averaged wave mean flow interaction in a rotating stratified incompressible flow [D.D. Holm and Y. Fukumoto (private communication)].

[2]R.R. Kerswell, "Elliptical instability," Annu. Rev. Fluid Mech. **34**, 83 (2002).

[3]Lord Kelvin, "Stability of fluid motion: Rectilinear motion of viscous fluid between two parallel plates," Philos. Mag. **24**, 188 (1887).

[4]B.J. Bayly, "Three-dimensional instability of elliptical flow," Phys. Rev. Lett. **57**, 2160 (1986).

[5]A.D.D. Craik and W.O. Criminale, "Evolution of wavelike disturbances in shear flows: A class of exact solutions of the Navier–Stokes equations," Proc. R. Soc. London, Ser. A **406**, 13 (1986).

[6]B.J. Guerts and D.D. Holm, "Alpha-modeling strategy for LES of turbu-

lent mixing,'' in *Turbulent Flow Computation*, edited by D. Drikakis and B.J. Geurts (Kluwer, New York, 2002), pp. 237–278.
[7]C. Foias, D.D. Holm, and E.S. Titi, ''The Navier–Stokes-alpha model of fluid turbulence,'' Physica D **152–153**, 505 (2001).
[8]B.R. Fabijonas and D.D. Holm, ''Mean effects of turbulence on elliptic instability,'' Phys. Rev. Lett. **90**, 124501 (2003).
[9]S. Chen, C. Foias, D.D. Holm, E. Olson, E.S. Titi, and S. Wynne, ''Camassa–Holm equations as a closure model for turbulent channel and pipe flow,'' Phys. Rev. Lett. **81**, 5338 (1998).
[10]S. Chen, C. Foias, D.D. Holm, E. Olson, E.S. Titi, and S. Wynne, ''The Camassa–Holm equations and turbulence in pipes and channels,'' Physica D **133**, 49 (1999).
[11]A.D.D. Craik, ''The stability of unbounded two- and three-dimensional flows subject to body forces: Some exact solutions,'' J. Fluid Mech. **198**, 275 (1989).
[12]A. Lifschitz, T. Miyazaki, and B.R. Fabijonas, ''A new class of instabilities of rotating flows,'' Eur. J. Mech. B/Fluids **17**, 605 (1998).
[13]M.J. Landman and P.G. Saffman, ''The three-dimensional instability of strained vortices in a viscous fluid,'' Phys. Fluids **30**, 2339 (1987).
[14]A. Lifschitz and B.R. Fabijonas, ''A new class of instabilities of rotating flows,'' Phys. Fluids **8**, 2239 (1996).
[15]F. Waleffe, ''On the three-dimensional instability of strained vortices,'' Phys. Fluids A **2**, 76 (1990).
[16]B.R. Fabijonas, D.D. Holm, and A. Lifschitz, ''Secondary instabilities of flows with elliptic streamlines,'' Phys. Rev. Lett. **78**, 1900 (1997).
[17]T. Miyazaki and A. Lifschitz, ''Three-dimensional instabilities of inertial waves in rotationg fluids,'' J. Phys. Soc. Jpn. **67**, 1226 (1998).
[18]V.A. Yakubovich and V.M. Starzhinskii, *Linear Differential Equations with Periodic Coefficients* (Wiley, New York, 1967).
[19]T. Miyazaki, ''Elliptical instability in a stably stratified rotating fluid,'' Phys. Fluids A **5**, 2702 (1993).
[20]C.G. Speziale, ''Analytical methods for the development of Reynolds-stress closures in turbulence,'' Annu. Rev. Fluid Mech. **23**, 107 (1991).
[21]J.E. Dunn and R.L. Fosdick, ''Thermodynamics, stability, and boundedness of fluids of complexity 2 and fluids of second grade,'' Arch. Ration. Mech. Anal. **56**, 191 (1974).
[22]R.S. Rivlin and J.L. Ericksen, ''Stress deformation relation for isotropic materials,'' J. Ration. Mech. Analysis **4**, 323 (1955).
[23]W. Noll and C. Truesdell, *The Nonlinear Field Theory of Mechanics. Handbook of Physik III* (Springer-Verlag, Berlin, 1975).
[24]R.S. Rivlin, ''The relation between the flow of non-Newtonian fluids and turbulent Newtonian fluids,'' Q. Appl. Math. **15**, 212 (1957).
[25]J. Leray, ''Sur le mouvement d'un liquide visqueux emplissant l'espace,'' Acta Math. **63**, 193 (1934).
[26]R.A. Clark, J.H. Ferziger, and W.C. Reynolds, ''Evaluation of subgrid-scale models using an accurately simulated turbulent flow,'' J. Fluid Mech. **91**, 1 (1979).
[27]A. Leonard, ''Energy cascade in large-eddy simulations of turbulent fluid flows,'' Adv. Geophys. **18**, 237 (1974).
[28]A.W. Vreman, B.J. Guerts, and J.G.M. Kuerten, ''Large eddy simulation of the temporal mixing layer using the Clark model,'' Theor. Comput. Fluid Dyn. **8**, 309 (1996).
[29]J. Bardina, J.H. Ferziger, and W.C. Reynolds, ''Improved turbulence models based on large eddy simulations of homogeneous incompressible turbulence,'' Technical Report No. TF-19, Stanford University, 1984.
[30]C. Cambon, J.P. Benoit, L. Shao, and L. Jacquin, ''Stability analysis and large-eddy simulation of rotating turbulence with organized eddies,'' J. Fluid Mech. **378**, 175 (1994).
[31]B.J. Geurts and D.D. Holm, ''Regularization modeling for large-eddy simulation,'' Phys. Fluids **15**, L13 (2003).
[32]B.J. Bayly, D.D. Holm, and A. Lifschitz, ''Three-dimensional stability of elliptical vortex columns in external strain flows,'' Philos. Trans. R. Soc. London, Ser. A **354**, 1 (1996).